

# Transmission Properties of One Dimensional Fractal Structures

H. Pashaei Adl and S. Roshan Entezar  
Faculty of Physics, University of Tabriz, Tabriz, Iran

Corresponding Author: [hamid.pashaei@gmail.com](mailto:hamid.pashaei@gmail.com)

**ABSTRACT—** In this paper, the optical properties of one dimensional fractal structures are investigated. We consider six typical fractal photonic structures: the symmetric dual cantor-like fractal structure, the asymmetric dual cantor-like fractal structure, the single cantor-like fractal structure, the symmetric dual golden-section fractal structure, the asymmetric dual golden-section fractal structure and the single golden-section fractal structure. By using the transfer matrix method the transmission spectra of these structures are simulated. The calculation results shows that the transmission spectrum of the symmetric dual cantor-like fractal structure is self-similar and the peak numbers in the transmission spectra of the SDGSFS also follow the principals of special fractal structures. It is also shown that in the symmetric dual golden-section fractal structure the localization of modes which appears within the stop band increases and getting closer to the middle of the gap by increasing the number of string.

**KEYWORDS:** Cantor like fractals, Golden section fractals, Transmission, Transfer matrix.

## I. INTRODUCTION

Problem of wave propagation in deterministic non-periodic inhomogeneous media such as quasi-crystals and fractal structures has attracted the attentions of researchers during the last decade [1-4]. This is due to the fact that many physical phenomena, natural structures and statistical processes can be analyzed and described by using a fractal approach [5-9]. From a mathematical point of view, the concept of fractal is associated with a geometrical object which: (1) is self-similar

(i.e., the object is exactly or approximately similar to a part of itself) and (2) has a fractional (or non-integer) dimension. Self-similar structures are obtained by performing a basic operation, called generator, on a given geometrical object called initiator. By repeating the process on multiple levels, in each one of them an object composed of sub-units of itself is created that resembles the structure of the whole object. Mathematically, this property should hold on all (infinite) scales. However, in the real world, there are necessarily lower and upper bounds over which such self-similar behavior applies. Moreover, as a consequence of fractals property, these structures exhibit a certain number of transmission peaks inside the frequency band gap. These systems have been analyzed using a transmission lines method. In this paper we consider six different fractal structures and analyze the properties of these fractal structures. Specially, we focus on the symmetric dual cantor-like fractal structure (SDCLFS), the asymmetric dual cantor-like fractal structure (ADCLFS), the single cantor-like fractal structure (SCLFS), the symmetric dual golden-section fractal structure (SDGSFS), the asymmetric dual golden-section fractal structure (ADGSFS) and the single golden-section fractal structure (SGSFS).

## II. THE THEORETICAL MODEL

### A. Performance of 1D Cantor-like Fractal Structures

The ID Cantor like fractal structure is obtained by dividing an initial string and repeating this

procedure to the last string (removing the center segment from three equivalent segments). This kind of fractal structures are classical fractals [14-16].

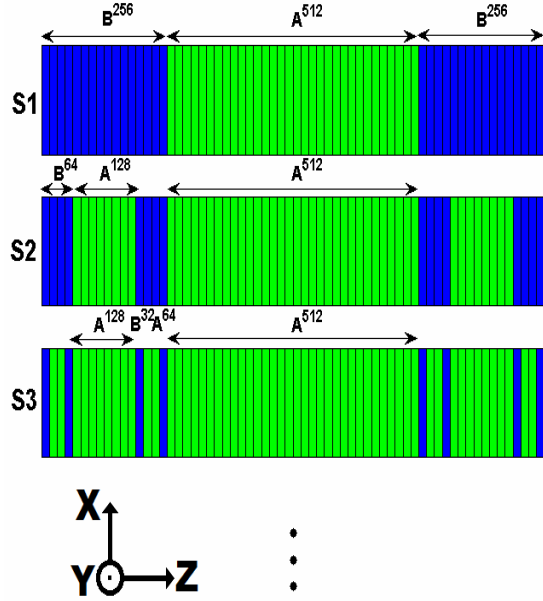


Fig. 1. Structure of the SDCLFS.

From the mathematical point of view, the fractal structure is started by deleting the open middle third  $[1/3, 2/3]$  from the interval  $[0, 1]$ , leaving two line segments:  $[0, 1/3] \cup [2/3, 1]$ . Next, the open middle third of each of these remaining segments is deleted, leaving four line segments:

$[0, 1/9] \cup [2/9, 1/3] \cup [2/3, 7/9] \cup [8/9, 1]$ . This process is continued ad infinitum, where the  $n$ th set:

$$C_n = \frac{C_{n-1}}{3} \cup \left( \frac{2}{3} + \frac{C_{n-1}}{3} \right) \quad (1)$$

Photonic fractals can resonate strongly electromagnetic waves with specific wavelength and use these waves in the self-similar structures of metallic or dielectric media. Such resonances have been observed in one-dimensional cantor fractals [17, 18], indeed the resonance can occur at different local levels of the self-similar structures at different frequencies.

Based on the Cantor fractal, we change the Cantor structure from BAB to other kinds of sets and create the cantor-like fractal structure (CLFS). The CLFS has two basic parameters: generator  $G$  and string  $S$ . Layer  $B$  is chosen as the seed layer, which is replaced by generator  $G$  when string  $S$  increases. By setting generator  $G=BAAB$  we can obtain the SDCLFS, which is shown in Fig. 1 with a different string  $S$ . While, by setting generator  $G=BABA$ , we can create ADCLFS, again based on two parameters which mentioned above (Fig. 2). When  $S=1$ , the SDCLFS consists of 4 parts  $B, A, A, B$  and also, ADCLFS consists of 4 parts  $B, A, B, A$  but the formation is different. In the first string, each part has 256 but when string ( $S$ ) increases to 2, each  $B$  part splits to 4 parts filled with  $B, A, A, B$  (or  $B, A, B, A$ ) respectively. Each new part has 64 layers. As this process goes on, when the string is  $S$ , the number of  $B$  parts is  $2^S$ , and each  $B$  part has a  $(1/4)^S$  ratio of total layers. As we known, the self-similarity dimension of a fractal is defined as:

$$D = \frac{\log(N)}{\log(r)} \quad (2)$$

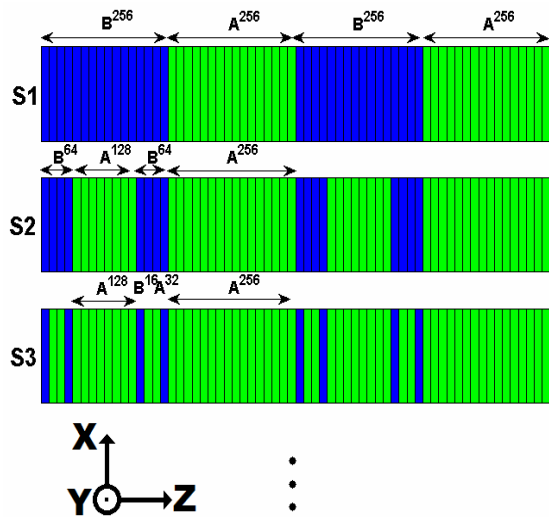


Fig. 2. Structure of the ADCLFS.

So the self-similarity of this kind of fractals can be calculated as

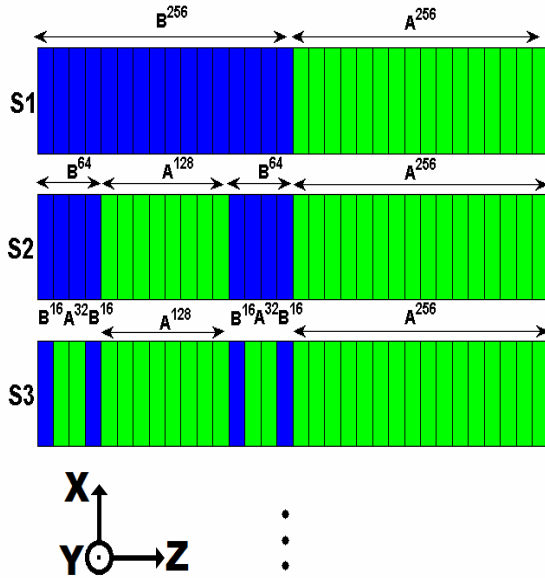


Fig. 3. Structure of the SCLFS.

$$D = -\log(N) / \log(r) = \log(2) / \log(4) = 0.5 .$$

By considering the generator as  $G=BA$ , one can obtain SCLFS as shown in Fig. 3.

**B. Performance of Golden-Section Fractal Structures**

In mathematics and the arts, two quantities are in the golden ratio ( $\varphi$ ) if the ratio of the sum of the quantities to the larger quantity is equal to the ratio of the larger quantity to the smaller one.

$$\frac{a+b}{a} = \frac{a}{b} \equiv \varphi \tag{3}$$

The researches show that the fractal dimensions in the nature always arrange from 1.6 to 1.7, which reminds us the golden section. For example, the fractal dimension of the golden spiral is about 1.619327, which is reflected in a seashell spiral, the tail of the sea horse, the leaves of plants, and so on. Also, many bones of humans are golden cut by a joint. Therefore, the golden section fractal is the result of biological evolution and natural selection [19, 20].

Studies show that the golden section exists not only in the biological world but also in other areas of nature such as quasi-crystals,

polymers, distances of planets, vortex waves, and so on. Thus, the golden section fractal is a most important phenomenon in nature.

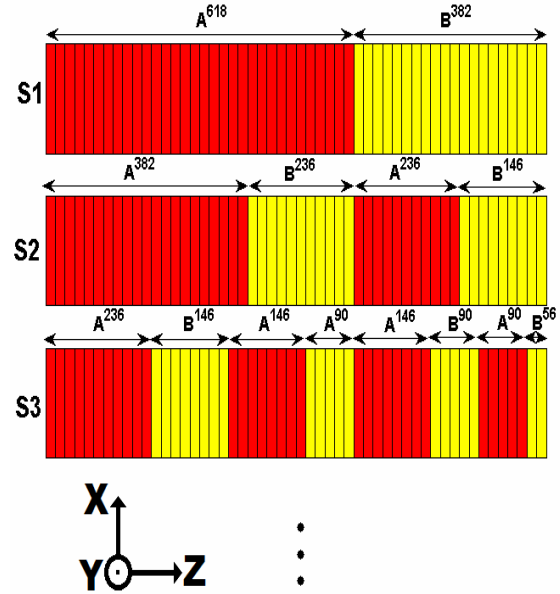


Fig. 4. Structure of the SDGSFS.

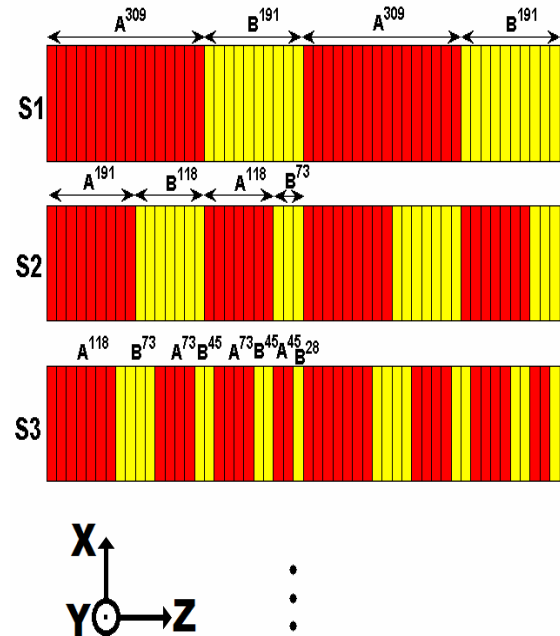


Fig. 5. Structure of the ADGSFS.

So it is interesting to investigate the optical properties of the 1D golden section fractal structures. We consider the SDGSFS and

ADGSFS which are shown in Fig. 4 and Fig. 5.

In the first string of the SDGSFS, the total number of golden layers is assigned to two parts, which are layers A and B, respectively. The number of layers in A is 618, and the number of layers in B is 382. In the second string of the SDGSFS structure, each part rearrange with A and B layers with regarding the golden ratio of the layer numbers. This process is continued ad infinitum. Then, we can get the nth string of the GSFS. As well as SDGSFS we considered the ADGSFS by attending to the golden ratio of layers number. To clarify the problem we also investigate the optical properties of the SGSFS (see Fig. 6).

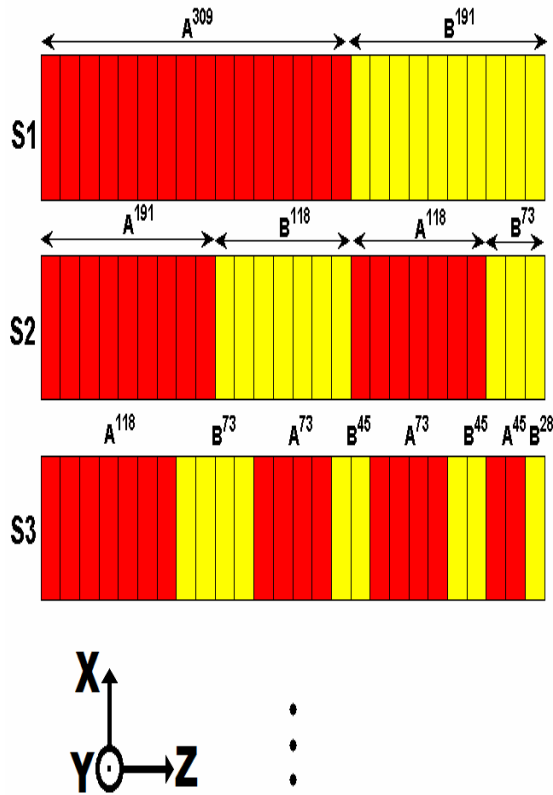


Fig. 6. Structure of the SGSFS.

**C. Basic Equations**

As shown above, the layers arrangement of the 1D fractal structures considered in this paper are in the following forms:

$$\begin{aligned}
 S_1 &: B^{256} (AA)^{256} B^{256} \\
 S_2 &: B^{64} (AA)^{64} B^{64} (AA)^{256} B^{64} (AA)^{64} B^{64} \\
 S_3 &: B^{16} (AA)^{16} B^{16} (AA)^{64} B^{16} (AA)^{16} B^{16} (AA)^{256} \dots \\
 &\dots B^{16} (AA)^{16} B^{16} (AA)^{64} B^{16} (AA)^{16} B^{16} \quad (4)
 \end{aligned}$$

for the SDCLFS (see Fig. 1),

$$\begin{aligned}
 S_1 &: \{B^{256} A^{256}\} \{B^{256} A^{256}\} \\
 S_2 &: \{B^{64} (AA)^{64} B^{64} A^{256}\} \{B^{64} (AA)^{64} B^{64} A^{256}\} \\
 S_3 &: \{B^{16} (AA)^{16} B^{16} (AA)^{64} B^{16} (AA)^{16} B^{16} A^{256}\} \dots \\
 &\dots \{B^{16} (AA)^{16} B^{16} (AA)^{64} B^{16} (AA)^{16} B^{16} A^{256}\} \quad (5)
 \end{aligned}$$

for the ADCLFS (see Fig. 2),

$$\begin{aligned}
 S_1 &: A^{618} B^{382} \\
 S_2 &: A^{382} B^{236} A^{236} B^{146} \\
 S_3 &: A^{236} B^{146} A^{146} B^{90} A^{146} B^{90} A^{90} B^{56} \\
 &\dots \quad (6)
 \end{aligned}$$

for the SDGSFS ( see Fig. 4) and

$$\begin{aligned}
 S_1 &: \{A^{309} B^{191}\} \{A^{309} B^{191}\} \\
 S_2 &: \{A^{191} B^{118} A^{118} B^{73}\} \{A^{191} B^{118} A^{118} B^{73}\} \\
 S_3 &: \{A^{118} B^{73} A^{73} B^{45} A^{73} B^{45} A^{45} B^{28}\} \dots \\
 &\dots \{A^{118} B^{73} A^{73} B^{45} A^{73} B^{45} A^{45} B^{28}\} \quad (7)
 \end{aligned}$$

for the ADGSFS (see Fig. 5). Here, A and B show the alternate dielectric layers,

respectively.  $S_i (i=1,2,\dots)$  represents the different string in the structures. In our study, the central wavelength is assumed to be  $\lambda_0 = 1550 \text{ nm}$  and the frequency can be obtained as  $\omega_0 = 2\pi c / \lambda_0$ , where  $c$  is the vacuum speed of light. The individual layers of the structures are considered as quarter-wave layers  $n_A d_A = n_B d_B = \lambda_0 / 4$  for which the quasi-periodicity is expected to be more effective. The refractive indices of the layers A and B are 1.41 and 2.3, respectively. Note that, in this paper, we only consider the case of transverse electric field. The electric fields in layers A and B are written as:

$$E_A(x, z) = E(z)e^{i(k_x x + k_{zA} z)} \hat{e}_y \quad (8)$$

$$E_B(x, z) = E(z)e^{i(k_x x + k_{zB} z)} \hat{e}_y \quad (9)$$

Here,

$k_{0x} = k_0 \sin(\theta)$ ,  $k_{zA} = k_0 \sqrt{\varepsilon_A \mu_A (1 - \sin^2 \theta / \varepsilon_A \mu_A)}$ ,  
 $k_{zB} = k_0 \sqrt{\varepsilon_B \mu_B (1 - \sin^2 \theta / \varepsilon_B \mu_B)}$ , with  $k_0 = \omega / c$ .  $\theta$  is the angle of the incident light. Also,  $\mu_A = \mu_B = 1$ ,  $\varepsilon_A = 1.9881$ ,  $\varepsilon_B = 5.29$ . Inside the layers, the electric field is governed by the Helmholtz equation [10]:

$$\frac{d^2 E}{dz^2} + (\varepsilon_j \mu_j \omega^2 / c^2 - k_x^2) E = 0 \quad (10)$$

The subscript 'j' denotes the number of the layers. At the interface between two layers, we can apply the boundary conditions:

$$\begin{aligned} E_+ &= E_- \\ \frac{1}{\mu_+} \frac{dE}{dz_+} &= \frac{1}{\mu_-} \frac{dE}{dz_-} \end{aligned} \quad (11)$$

Therefore, by applying the boundary conditions in the interfaces between layers we can employ the transfer matrix to combine the electric field at  $z$  and  $z + \Delta z$  [10-13]:

$$m_i(\Delta z_i) = \begin{bmatrix} \cos(k_{zi} \Delta z_i) & -\frac{\mu_i \omega}{k_{zi} c} \sin(k_{zi} \Delta z_i) \\ \frac{k_{zi} c}{\mu_i \omega} \sin(k_{zi} \Delta z_i) & \cos(k_{zi} \Delta z_i) \end{bmatrix} \quad (12)$$

here,  $i = A, B$ ,  $\Delta z_A = d_A$ ,  $\Delta z_B = d_B$  and  $l = 1, \dots, N$ , where  $N$  is the total number of the layers in the fractal structure. And finally, we have the global transfer matrix:

$$M^g = \prod_{l=1}^N m_l(\Delta z_l) \quad \text{whre } i = A, B \quad (13)$$

The tangential components of the electric and magnetic fields at incident side ( $z = 0$ ) and the transmitted side ( $z = L$ ) are related by the following matrix equation:

$$\begin{pmatrix} E_{y1} \\ H_{y1} \end{pmatrix}_{z=0} = M^g \begin{pmatrix} E_{yN} \\ H_{yN} \end{pmatrix}_{z=L} \quad (14)$$

Finally, the transmission can be obtained as  $T = tt^*$  where  $t = 2p / (pM_{11}^g + pM_{22}^g + p^2 M_{12}^g + M_{22}^g)$  and  $p = \cos(\theta)$ .

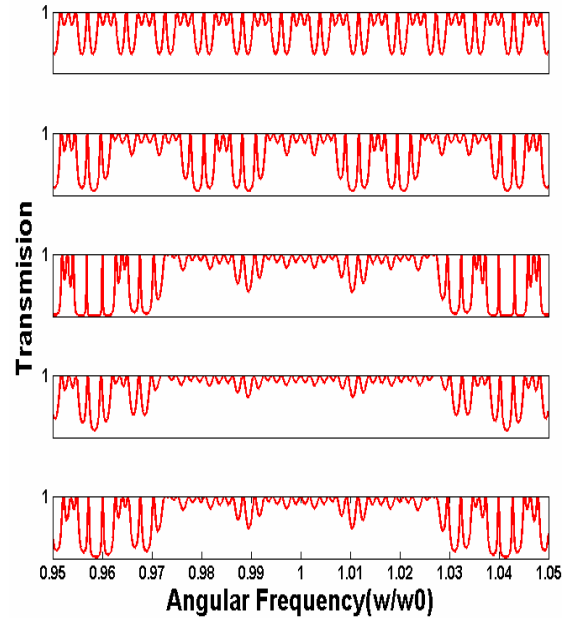


**Fig. 7.** Transmission spectrum of the SDCLFS with string S ranging from 1 to 5 at normal incidence with  $d_A = \frac{\lambda_0}{4n_A}$ ,  $d_B = \frac{\lambda_0}{4n_B}$ .

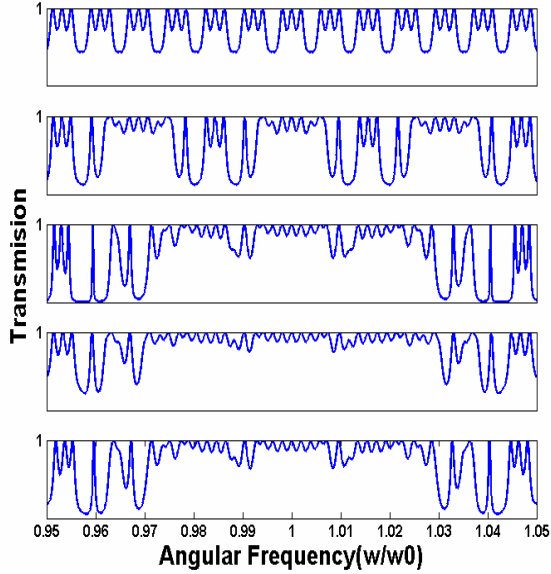


**Fig. 8.** Transmission spectrum of the ADCLFS with string S ranging from 1 to 5 at normal incidence with  $d_A = \frac{\lambda_0}{4n_A}$ ,  $d_B = \frac{\lambda_0}{4n_B}$ .

### III. NUMERICAL SIMULATIONS

The transmission spectrum of the SDCLFS and ADCLFS are shown in Figs.7 and 8. The self-similarity property is the most important characteristic of the fractal structure. A self-similar object is exactly or approximately similar to a part of itself (i.e., the whole has the same shape as one or more of the parts). Self-similarity is a typical property of the fractals. We can easily observe the self-similar property in the transmission spectrum of the SDCLFS and ADCLFS. Admittedly, the self-similarity is clearly seen in both of these structures (CLFS and DCLFS) but by increasing the number of string in any of them the structures graphs fluctuated gently around the maximum transmission. To illustrate this property, the transmission spectrum of the SCLFS is shown in Fig. 9.

In continue we investigate the transmission properties of the SDGSFS and ADGSFS with different string number and plot the transmission spectra in Figs.10 and 11, respectively. Figure 10 with S=1 describes the transmission spectrum of the first string of the

SDGSFS, the main transmission peak in the central frequency is a sole peak.

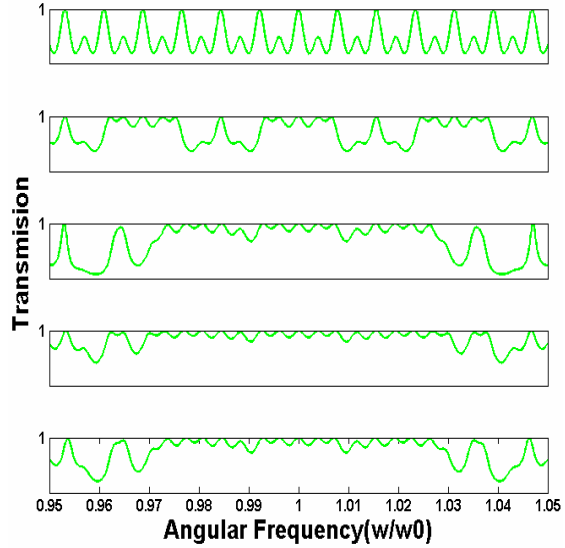


**Fig. 9.** Transmission spectrum for the SCLFS with string S ranging from 1 to 5 at normal incidence with  $d_A = \frac{\lambda_0}{4n_A}$ ,  $d_B = \frac{\lambda_0}{4n_B}$ .

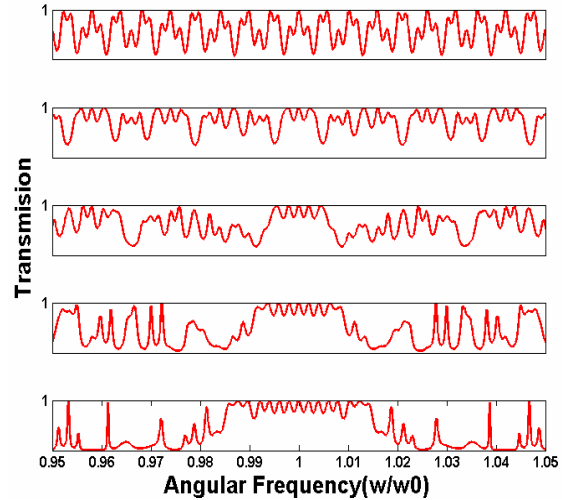


**Fig. 10.** Transmission spectrum of SDGSFS with string S ranging from 1 to 5 at normal incidence with  $d_A = \frac{\lambda_0}{4n_A}$ ,  $d_B = \frac{\lambda_0}{4n_B}$ .

The transmission spectrum of the second string of the SDGSFS is shown in Fig. 10 (S=2) that main transmission peak in the center frequency is made up of 3 small side-bands. And for the third string of the GSFS is made up of 5 small side-bands and so on. We can prove the rule

that the main transmission peak of the SDGSFS will have more sidebands when string S increases.

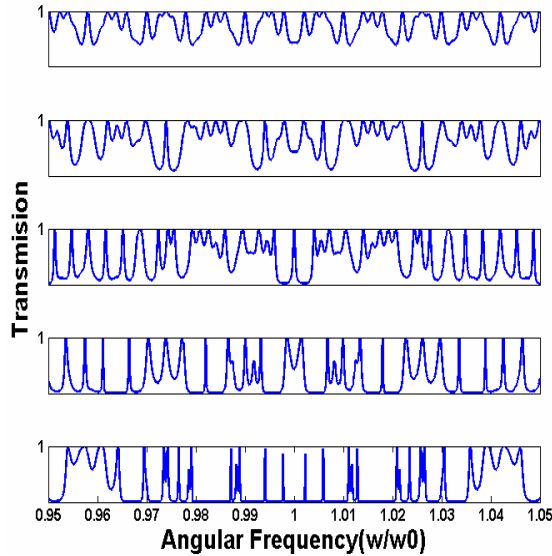


**Fig. 11.** Transmission spectrum of SDGSFS with string S ranging from 1 to 5 at normal incidence with  $d_A = \frac{\lambda_0}{4n_A}$ ,  $d_B = \frac{\lambda_0}{4n_B}$ .

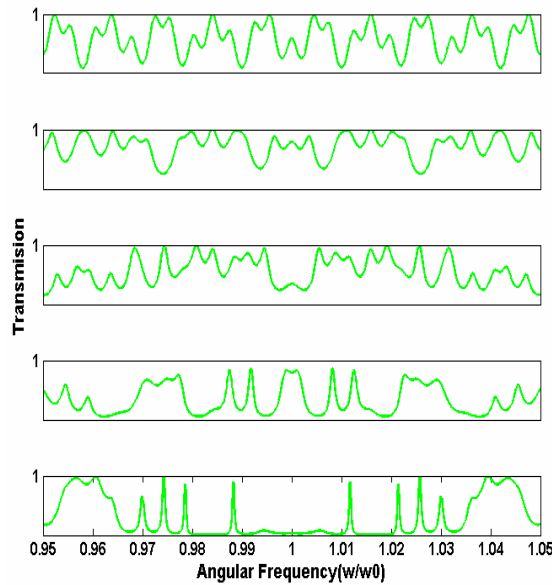


**Fig. 12.** Transmission spectrum for half of ADGSFS with string S ranging from 1 to 5 at normal incidence with  $d_A = \frac{\lambda_0}{4n_A}$ ,  $d_B = \frac{\lambda_0}{4n_B}$ .

By analyzing the transmission spectrum of ADGSFS (Fig. 11) one can see that, the stop band which the transmission modes appear inside it, widen and localization of the modes

increase and they get closer to the center of the stop band by increasing the number of string. Same as the case of SDGSFS, we can prove a rule that the localization of modes will increase by increasing the number of string.

Due to the rule that mentioned above about the localization of modes, the SGSFS structures have been studied and results verified this rule (see Fig. 12).

#### IV. CONCLUSION

In this paper the optical properties of some fractal structures has been investigated. First, we designed the symmetric dual cantor-like fractal structure, asymmetric cantor-like fractal structure and the single cantor-like fractal structure; and simulated their transmission spectrum. The simulation results showed an interesting rule. This rule says that the self-similarity of the fractal structure can form a self-similar transmission spectrum which by increasing the number of string, the diagrams fluctuates around the maximum transmission gently. Then, the transmission properties of the symmetric dual golden section fractal structure, the asymmetric dual golden section fractal structure and the single golden section fractal structure have been analyzed. In the symmetric dual golden-section structure the number of side-bands in the main peak of the transmission spectrum depends on the string number. Also, in the asymmetric dual golden-section structure the position of the modes that appears in the stop band depend on the string number; and their localization increases by increasing the string number.

#### REFERENCES

- [1] E. Macia, "Optical engineering with Fibonacci dielectric multilayers," *Appl. Phys. Lett.* Vol. 73, pp. 3330-3332, 1998.
- [2] M. Kohmoto and B. Sutherland, "Critical wave functions and a Cantor- set dimensional quasicrystal model," *Phys. Rev. B*, Vol. 35, pp. 1020-1033, 1987.

- [3] N. Liu, "Propagation of light waves in Thue-Morse dielectric multilayers," *Phys. Rev. B*, Vol. 55, pp. 3543-3547, 1997.
- [4] M.S. Vasconcelos, E.L. Albuquerque, and A.M. Mariz, "Optical localization in quasi-periodic multilayers," *J. Phys: Cond. Matt*. Vol. 10, pp. 5839-5849, 1998.
- [5] A. Hunt, N. Gershenzon, and G. Bambakidis, "Computational and Experimental study of the Fractal Behavior of Rock Surfaces," *Tect. Phys.* Vol. 431, pp. 23-32, 2007.
- [6] D. Perugini, A. Speziali, L. Caricchi, and U. Kueppers "Application of fractal fragmentation theory to natural pyroclastic deposits: Insights into volcanic explosivity of the Valentano scoria cone (Italy)," *J. Volc. and Geoth. Res.* Vol. 202, pp. 200-210, 2011.
- [7] B.J. West and D.R. Bickel "Molecular evolution modeled as a fractal stochastic process," *Physica A*, Vol. 249, pp. 544-552, 1998.
- [8] M.R. Schure and J.M. Davis "The statistical overlap theory of chromatography using power law (fractal) statistics," *J. Chrom. A*, Vol. 1218, pp. 9297-9306, 2011.
- [9] B.B. Mandelbrot, *The Fractal Geometry of Nature*, Freeman, San Francisco, Calif. 1982.
- [10] S.M. Wang and L. Gao, "Nonlinear responses of the periodic structure composed of single negative materials" *Opt. Commun.* Vol. 267, pp. 197-204, 2006.
- [11] N.H. Liu, S.Y. Zhu, H. Chen, and X. Wu, "Superluminal pulse propagation through one-dimensional photonic crystals with a dispersive defect," *Phys. Rev. E* 65, 046607-446617, 2002.
- [12] L.G. Wang, N.H. Liu, Q. Lin, and S.Y. Zhu, "Propagation of coherent and partially coherent pulses through one-dimensional photonic crystals," *Phys. Rev. E*, Vol. 70, pp. 016601-016612, 2004.
- [13] M. Zulfiqar Ali and T. Abdullah, "Properties of the angular gap in a one-dimensional photonic band gap structure containing single negative materials," *Phys. Lett A*, Vol. 372, pp. 1695-1700, 2008.
- [14] D.J. Feng, H. Rao, and J. Wu, "The net measure properties for symmetric Cantor sets and their applications," *Prog. Nat. Sci.* Vol. 7, pp. 172-178, 1997.
- [15] S. Corvise and M. Rams, "IFS attractors and Cantor sets," *Topol. Appl.* Vol. 153, pp. 1849-1859, 2006.
- [16] M. Dai and L. Tian, "The structure of a Cantor-like set with overlap," *Chaos, Solitons Fractals*, Vol. 26, pp. 295-301, 2005.
- [17] X. Sun and D.L. Jaggard "Wave Interactions with Generalized Cantor Bar Fractal Multilayers," *J. Appl. Phys.* Vol. 70, pp. 1131-1143, 1991.
- [18] Y. Miyamoto, H. Kanaoka, and S. Kiriara "Terahertz wave localization at a three-dimensional ceramic fractal cavity in photonic crystals," *J. Appl. Phys.* Vol. 103, pp. 103106-103111, 2008.
- [19] H. Walser and P. Hilton "The golden section," *Math. Assoc. of Am.* 2001.
- [20] A. Arneodo, F. Argoul, E. Bacry, J.F. Muzy, and M. Tabard, "Golden mean arithmetic in fractal branching of diffusion-limited aggregates" *Phys. Rev. Lett.* Vol. 68, pp. 3456-3459, 1992.



**Hamid Pashaei Adl** was born in Bonab, Iran, in 1985. He received his M.Sc. degree in Physics (Atomic and Molecular- Laser) from University of Tabriz, Tabriz, Iran, in 2011. He has cooperated with Dr. Roshan Entezar Research Group in Physics Department of University of Tabriz as a guest researcher. His current research activities are in the fields of Photonic Crystals, Linear and Nonlinear Optics in Photonic Crystal and Metamaterial.



**Samad Roshan Entezar** was born in Tabriz, Iran, in 1969. He received the M.S. degree in physics (atomic and molecular) and the Ph.D. degree in laser physics from university of Tabriz, Iran, in 2001 and 2006, respectively. In 2007, he joined the Physics Department of university of Tabriz as an assistant professor of Physics. His current research activities are in the fields of quantum optics in photonic crystals, linear and nonlinear optics in photonic crystal and metamaterial. Dr. Roshan Entezar has authored and coauthored more than 30 scientific papers in peer-referred international journals.

**THIS PAGE IS INTENTIONALLY LEFT BLANK.**